Low-Cost Flywheel Energy Storage for Mitigating the Variability of Renewable Power Generation

Investigators
The University of Texas at Austin
Dr. Robert Hebner, Director/Principal Investigator, Center for Electromechanics;
Dr. Siddharth Pratap, Senior Research Scientist, Center for Electromechanics;
Mr. Michael Lewis, Program Manager, Center for Electromechanics;
Mr. Clay Hearn, Research Engineer/Graduate Researcher, Center for Electromechanics.

Abstract

In the past year, the researchers at the Center for Electromechanics at The University of Texas at Austin (UT-CEM) and the Nanotech Institute at The University of Texas at Dallas (UTD) concluded research efforts on improved flywheel designs and flywheel materials to meet energy storage requirements for the grid.

UT-CEM's efforts focused on developing design codes and methods for incorporating high temperature superconducting (HTSC) materials into flywheel bearing designs. The driving principle behind HTSC bearings is the stable levitation of permanent magnet material due to induced pinning currents in bulk superconductors. Such bearings can provide low loss rates of up to 0.1% stored energy per hour, which would make diurnal energy storage applications with flywheels practical. This development has resulted in lumped parameter models that were proven and verified against laboratory experiments and finite element models. The lumped parameter methodology will aid in the design and characterization of HTSC bearings for high speed flywheel rotors.

In this past year, UT-CEM used their design code and material results from UT-Dallas to study the potential impact of these advanced technologies for flywheel energy storage. These results showed that significant improvements could be made to energy storage density utilizing magnetically filled nano-composites in the flywheel bearing design.

Introduction

The purpose of the research and development program was to investigate game-changing technologies and materials to advanced flywheel kinetic energy storage for utility grid applications. The goal was to store 50% of the grid capacity within 50 years. Since flywheels are mechanical energy storage devices, very high cycle lives, up to and above 1 million cycles with proper design, can be achieved with little to no loss in performance degradation. Key advances have been made which should keep us on the path to reaching that goal.

Previous work at the University of Texas at Austin evaluated flywheel sizing requirements for different locations within the utility grid. Typically, flywheels have been used for high power - low energy storage applications such as frequency and voltage regulation where energy storage devices with high cycle life are required [1]. For longer term energy storage applications, flywheels suffer frictional losses which are due to

windage and bearings. Windage losses can be significantly reduced by operation at vacuum levels below 1 mTorr, which are achievable for stationary grid utility applications. Currently, most high performance flywheels operate with contactless active magnetic bearings. Although there is no mechanical contact with these bearings, magnetic hysteresis and eddy current generation in the laminations can still produce loss rates of up to 5% stored energy per hour [2], [3]. For the technology to be viable to assist in the incorporation of large scale storage in the electrical grid, those losses must be reduced by more than a factor of ten.

High temperature superconducting (HTSC) bearings show promise for making it possible to achieve this efficiency goal. The driving principle behind HTSC bearings is the stable levitation of permanent magnet material due to induced pinning currents in bulk superconductors. Such bearings can provide low loss rates of up to 0.1% stored energy per hour, [4], [5], which would make diurnal energy storage applications with flywheels practical. Although stable, the force-displacement interaction between a permanent magnet and sub-critical superconductor is highly nonlinear and has a well known hysteretic behavior. The University of Texas at Austin has developed lumped parameter modeling techniques for the design and characterization of HTSC bearings for high speed flywheel rotors.

Results

Over the course of the GCEP program, UT-Austin has developed techniques for designing high temperature superconducting bearings for flywheel energy storage systems. These modeling techniques significantly reduce computational time over high level finite element methods without sacrificing nonlinear hysteresis and losses that occur between a levitated permanent magnet-bulk HTSC system. Bearing designs can be faster with these developed techniques, and investigations can be performed to determine material requirements for specific applications.

Dynamic Validation of Lumped Parameter Model

Further testing has been performed to validate the 3D lumped parameter model, that predicts the translational and vertical forces of a levitated permanent magnet over a bulk HTSC. This model is useful for estimating the radial bearing stiffness of a HTSC bearing design, along with coupled axial forces. Bearing stiffness is a critical parameter for stable system operation. To validate the model, a frequency response test was constructed, which permitted the determination of local stiffness coefficients, that are critical for characterizing rotor dynamic behavior.

The test setup is shown in Figure 1, in which a linear stepper motor was used to give either a step displacement to the superconducting base, or a random input signal to shake the superconducting base. Laser displacement sensors, LDS's, were used to measure the displacement of the base and the displacement of the levitated magnet, which was embedded in a G10 carrier.

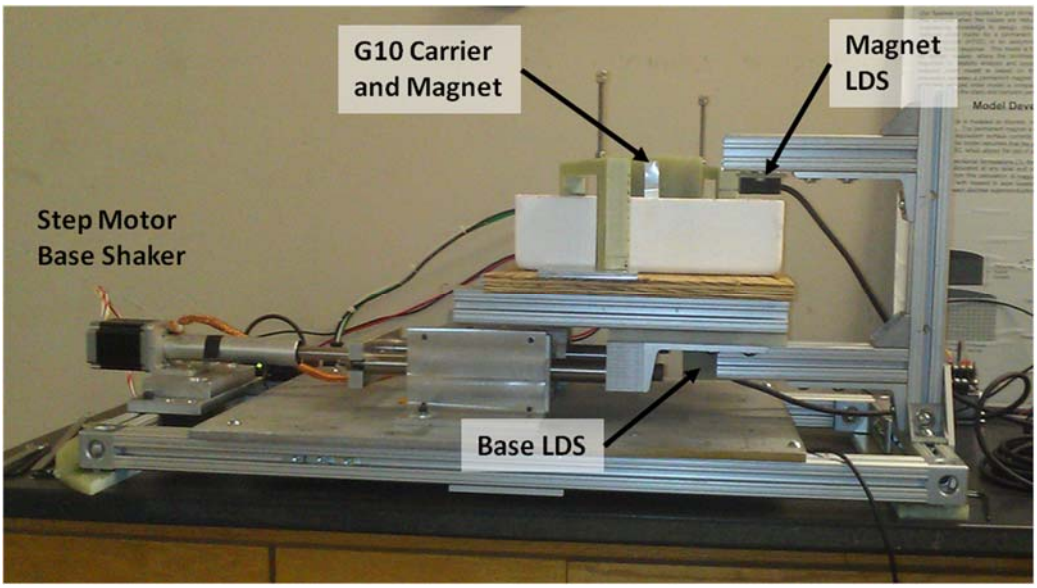

Figure 1: Test setup for dynamic transverse model validation

For the dynamic transverse test, a larger HTSC test bearing setup was constructed. The HTSC base consisted of 6 bulk YBCO superconductors provided by Adelwitz Technologiezentrum that have an expected critical current density of 10 to 100 kA/cm^2 [6]. The rectangular bulk superconductors each measured on average 67 mm L x 35 mm W x 13 mm H and were assembled to produce a base which was approximately 134 mm L x 105 mm W. These bulk superconductors were produced by using three different seed locations, which means each block has three separate crystals, and grain boundaries in between. The grain boundaries can impede bulk current flow in the superconducting material and constrain current paths [7]. The superconductors were bonded to a sheet of G10 plate and placed in a cryostat, Figure 2.

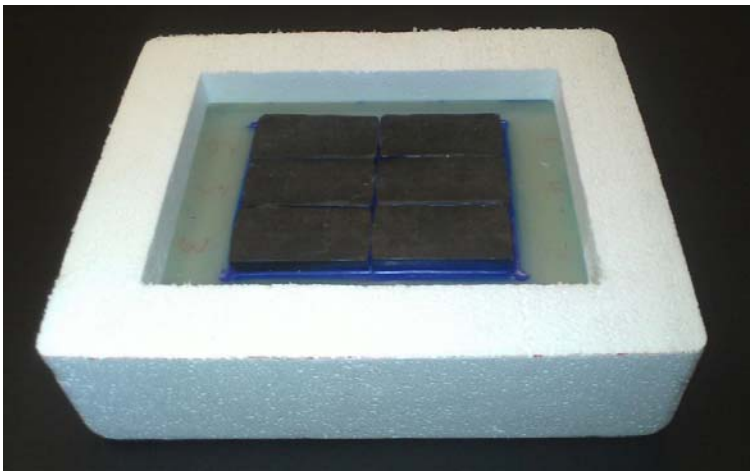

Figure 2: Base of bulk YBCO superconductors for dynamic transverse test

A larger permanent magnet was also used for the dynamic test setup. A high strength, N42, neodymium magnet was used, that measured 76.2 mm OD x 50.8 mm ID x 25.4 mm H. The field strength of the magnet at the surface was measured at 0.51 T, which correlates to a coercive strength of 1030 kA/m. The magnet was bonded into a G10 carrier, that measured 114.3 mm OD x 50.8 mm H, and provided the system with some additional mass, Figure 3. The magnet and G10 carrier had a net mass of 1.292 kg.

Figure 3 Permanent magnet bonded in G10 carrier for dynamic test.

For the test, the permanent magnet was initially centered and positioned 2 mm above the surface of the bulk YBCOs in the cryostat. Measured spacers were used to maintain this height during field cooling. Once the magnet was positioned, liquid nitrogen was then added to the cryostat to bring the temperature down below critical, at which time, the spacers were removed to allow the permanent magnet assembly to freely levitate.

The first tests evaluated system response to a step input. For these tests, the stepper motor quickly moved the YBCO base forward 1 mm, and the LDS probes measured the displacement of both the base and G10 carrier. A sample rate of 1000 Hz was used for data collection, and data was passed through a 100 Hz, 2nd order, Butterworth low pass filter to reduce noise. The time domain response to the step input shows significant damping in the system. This high level of damping was not expected to occur between the permanent magnet and bulk superconductor. This damping could be a product of viscous friction between the permanent magnet and the surrounding liquid nitrogen. An FFT (fast Fourier transform) of the damped response shows a peak response at 19.6 Hz.

For the lumped parameter model, the YBCO blocks of the HTSC bearing plate are modeled by discrete, overlapping superconducting discs that couple permanent magnet displacement to induced voltages per Faraday's law of induction. The disc mesh of the HTSC plate was modeled as 18 discrete bulk superconducting regions, which considers the 6 individual YBCO blocks and 3 grain crystals per block, as shown in Figure 4. This type of mesh prevents bulk current flow between blocks and grains within the bulk YBCO to better replicate current flow.

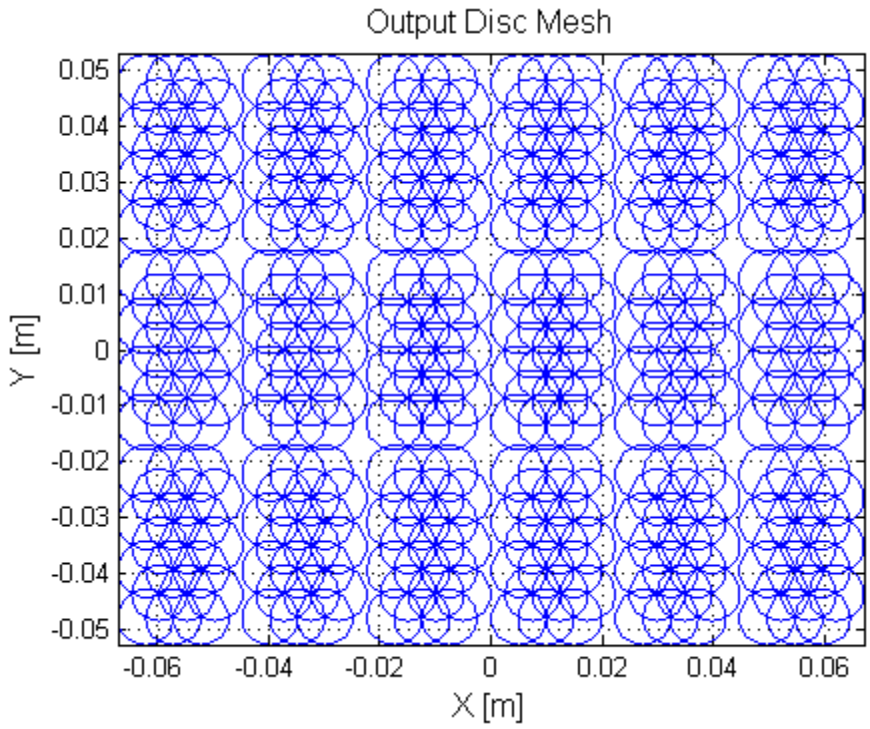

Figure 4: Updated mesh of bulk superconductors based on meshing individual grains

Input base measurements from the step input and shaker tests were used with the lumped parameter model to assess model performance. The following set of dynamic equations (1) were used to simulate the motion of the magnet, where x_m and v_{m_x} are state variables of the translational magnet position and translational velocity. Motion of the permanent magnet in the vertical direction is also captured by the state variables z_m and v_{m_z}.. The inputs x_b and v_b refer to the position and velocity of the YBCO base, which comes from the recorded data. Although the base position is only recorded, the base velocity was estimated by the position differential between time steps. The gyrator moduli for the model, $\frac{d\phi}{dq}$, are calculated based on the magnet field strength and the differential distance between the magnet and base, $(x_m - x_b)$, and the vertical position of the magnet. An additional damping term, B, is added to the set of dynamic equations to add additional losses which may come from viscous friction between the liquid nitrogen and magnet, as observed by the damp step response from the data.

$$\dot{x}_m = v_{m\_x}(t)$$

$$\dot{v}_{m\_x} = -\frac{B}{M} v_{m\_x} + \frac{1}{M}\left(\sum_{j=1}^{N} \frac{d\phi_j(x_m, x_b, z_m)}{dx} I_j\right) \tag{1}$$

$$\dot{z}_m = v_{m\_z}(t)$$

$$\dot{v}_{m\_z} = -g + \frac{1}{M}\left(\sum_{j=1}^{N} \frac{d\phi_j(x_m, x_b, z_m)}{dz} I_j\right)$$

$$\begin{bmatrix} \frac{dI_1}{dt} \\ \frac{dI_2}{dt} \\ \vdots \\ \frac{dI_N}{dt} \end{bmatrix} = -\boldsymbol{L}^{-1}\left[\begin{bmatrix} e_1 \\ e_2 \\ \vdots \\ e_N \end{bmatrix} + \begin{bmatrix} \frac{d\phi_1(x_m, x_b, z_m)}{dx} \\ \frac{d\phi_2(x_m, x_b, z_m)}{dx} \\ \vdots \\ \frac{d\phi_N(x_m, x_b, z_m)}{dx} \end{bmatrix}(v_x - v_b) + \begin{bmatrix} \frac{d\phi_1(x_m, x_b, z_m)}{dz} \\ \frac{d\phi_2(x_m, x_b, z_m)}{dz} \\ \vdots \\ \frac{d\phi_N(x_m, x_b, z_m)}{dz} \end{bmatrix} v_{m\_z}\right]$$

The lumped parameter model was solved with a fixed step 4th order Runge Kutta solver, using a time step of 1 ms, over the 2 s duration of the test. The total solution time was under 2 minutes, on a 64 bit desktop computer, which is significantly faster than a high level FEM analysis. The FEM approach may take over a day of computational time to solve for a single oscillatory cycle. Figures 5 and 6 shows the time domain and FFT comparison responses of the bearing reaction to a 1 mm step input. Evaluation of the test results showed a frequency response of 19.6 Hz, whereas the lumped parameter model predicted a slightly higher frequency of 20.6 Hz, which is within 5% of the observed value.

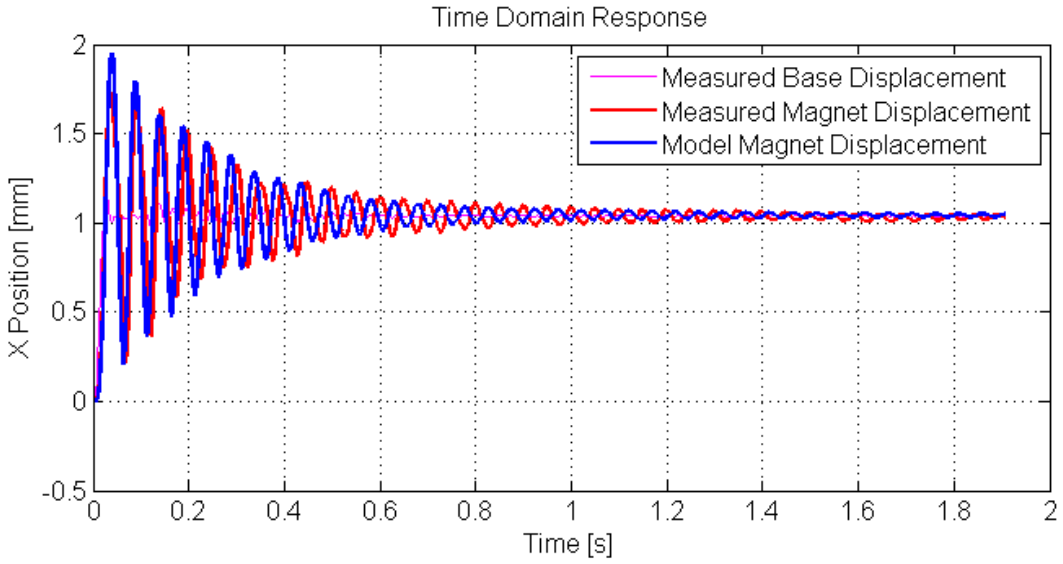

Figure 5: Time domain step response of lumped parameter model using grain mesh with additional viscous damping

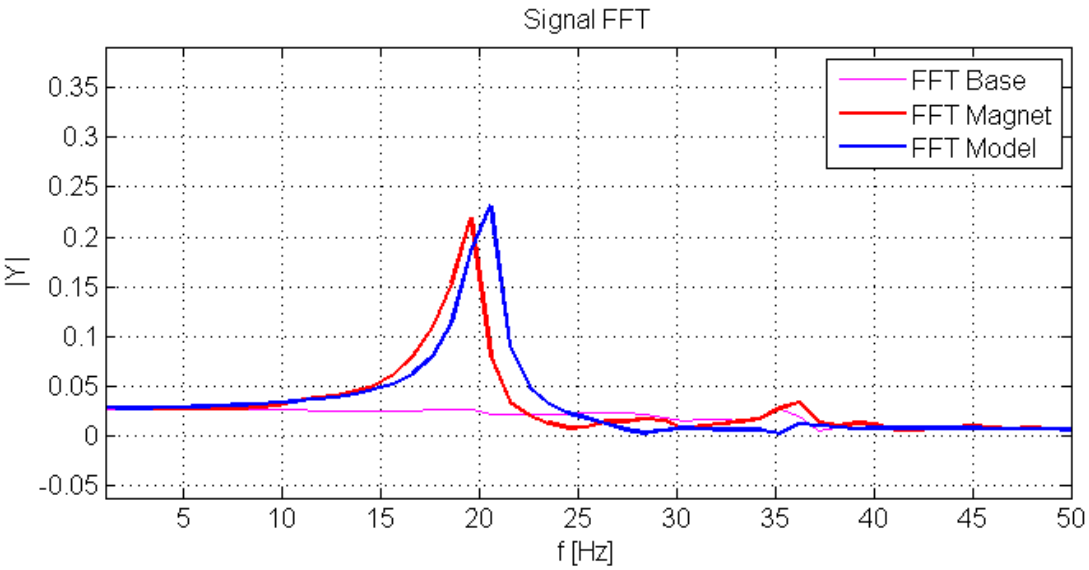

Figure 6: FFT step response of lumped parameter model using grain mesh technique with additional viscous damping

Application to Bearing Design and Advanced Materials

The modeling tools developed by UT-CEM under the GCEP program significantly reduce computational effort and allow trade studies to be performed which can quickly evaluate different bearing designs and materials. In collaboration with UT-CEM, UT-Dallas is investigating the development of embedded magnetic material within graphite composite bandings utilizing their developed techniques for biscrolling carbon-nanotube forests.

Current HTSC bearing constructions use individual permanent magnet pieces, [8], [9], which have no hoop continuity and contribute to significant mass loading on the flywheel composite bandings. In addition to mechanical performance, the lack of mechanical continuity circumferentially around the bearing also means the magnetic field generated by the permanent magnet rings are not continuous circumferentially. Changes in the magnetic field in this direction induce losses in the bearing system and degrades performance [10]. Advanced carbon-composite magnetic bandings would have higher hoop structural integrity to withstand spin loads and limit spin growth, along with a more uniform magnetic field, that will further reduce losses.

Currently, high strength neodymium permanent magnets can reach coercive strengths above 950 kA/m to produce fields above 1.2 T. It is reasonable to expect that a magnetic composite bandings will be unable to reach the magnetic performance of current high strength neodymium magnets due to the rule of mixtures. This decreased magnetic strength will reduce the bearing performance and limit lifting capacity. To evaluate the impact of decreased magnetic performance on lifting capacity, an analysis of a journal bearing design with the reduced order axissymmetric model was performed.

A journal bearing is shown in Figure 7 for a flywheel design where the permanent magnet material is located inside the ID hub of high strength composite bandings (rotating component), and an array of bulk high temperature superconductors is located on the stator side. The magnetic material is arranged in two pole pairs, as shown in Figure 7, for this particular design. Typically, the permanent magnets for an HTSC bearing design will be arranged in alternating pole pairs, or as a Halbach array to increase magnetic field gradients and bearing force [8], [6].

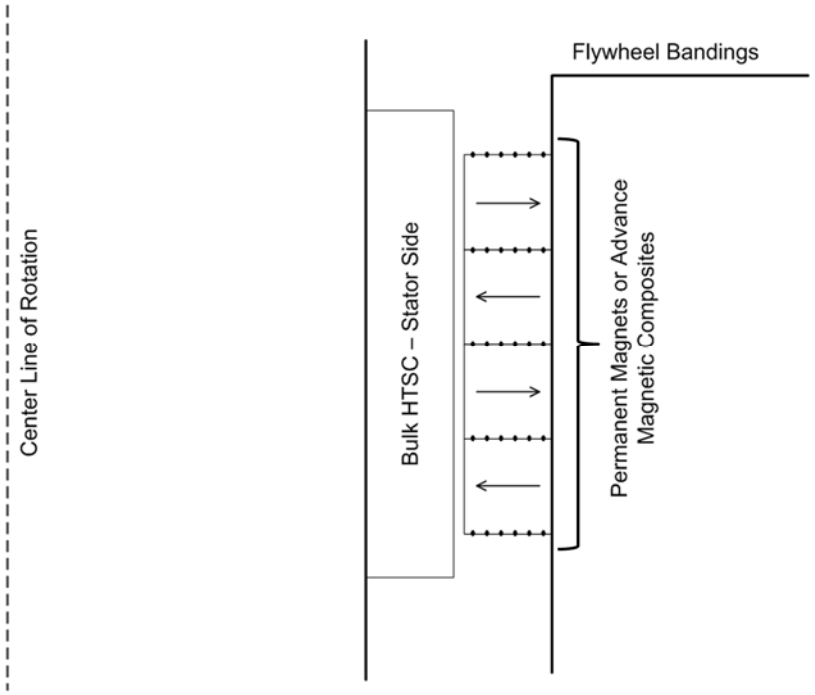

Figure 7: Axissymmetric view of typical HTSC journal bearing design

To evaluate the decreased magnetic performance on lifting capability, the axisymmetric model was used to evaluate the proposed bearing design. For this analysis, the bearing geometry was kept constant, and only the coercive strength of the permanent magnet material was changed to reflect performance of the magnetic composite banding. The magnetic material was located on the inside bore of a 350 mm ID composite banding. The material had an axial span of 100mm and was 25mm thick, in the radial direction. The bulk HTSCs on the stator side had a radial thickness of 15 mm and an axial length of 130 mm. A 1 mm air gap between the magnets and bulk HTSC was assumed for this design. The bulk HTSCs had an assumed critical current density, *Jc*, of 12 kA/m^2, which is achievable with current YBCO material, [6].

An axial sweep of the permanent magnets from +/- 100mm was analyzed to determine the amount of axial force generated by the bearing assembly. This procedure of sweeping the magnets pass the bulk HTSC is required to induce currents within the bulk HTSC, that will provide the levitation forces for the bearing assembly. The reduced order axissymmetric model, developed by UT-CEM under the GCEP program, was used

to evaluate these for potential magnetic materials [11]. Coercive magnetic strengths ranging from 930 kA/m to 515 kA/m were evaluated, where 930 kA/m is representative of full strength neodymium permanent magnets. Work performed by UT-Dallas has demonstrated magnetic composites using carbon nano-tubes in the range of 207 - 676 kA/m.

Results for this study are shown in Figure 8, where the peak axial force is normalized against the surface area of the permanent magnets to yield a peak levitation shear stress. This normalization allows these results to be extrapolated to different size bearing designs. For a full strength magnet, this analysis predicts a maximum levitation pressure of 74 kPa. For a magnetic performance of 515 kA/m, the levitation shear pressure is reduced to 21 kPa. This result indicates that for a 44.4% reduction in magnetic strength, the lifting capacity will be reduced by 71.0%. In order to make up for the reduced lifting capacity, a larger bearing area will be required, which may also limit the geometry for potential flywheel designs (i.e. preference towards elongated flywheels).

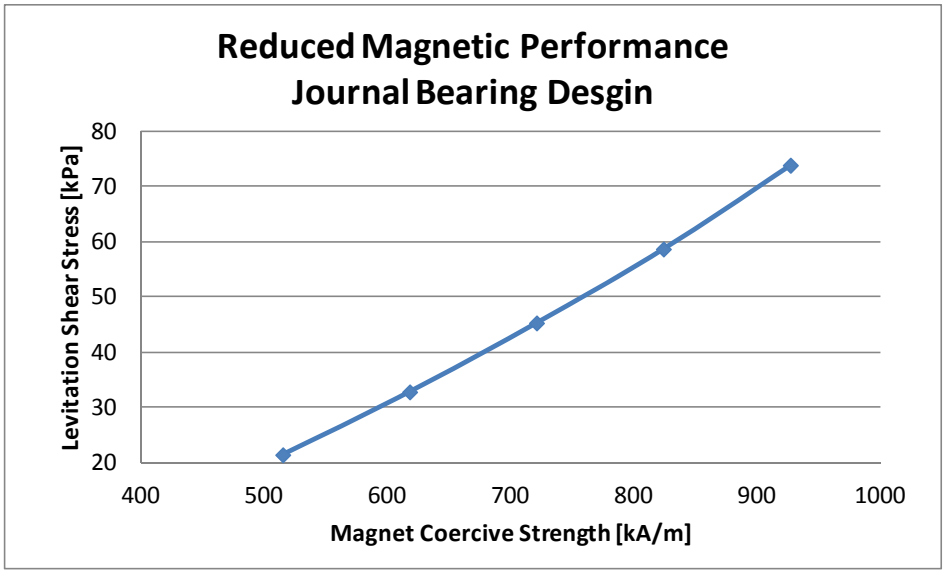

Figure 8: Analysis using lumped parameter axisymmetric model for estimating reduction in journal bearing lifting capacity with reduced magnetic performance

The advantage to using magnetic carbon composites for magnetic bearings will come with structural performance. High strength permanent magnets are brittle and lack the strength to withstand the high hoop stresses due to spin loads. Due to these mechanical limits, along with manufacturing limits, the permanent magnet side of a conventional HTSC bearing would be fabricated from individual permanent magnet arc segments. This non-continuous structure would lack hoop integrity and avoid damaging internal stresses, but the mass of the structure is now fully supported by the surrounding composite bandings. The mass loading of the permanent magnet assembly against the composite bandings becomes a design constraint that limits the performance of potential flywheel designs.

A circumferentially continuous composite banding with magnetic properties could reduce the mass loading against the supporting composite bandings and allow the flywheel to reach higher speeds and energy storage potentials. Two potential point designs were analyzed through 1-D nested ring analysis to determine potential improvements to flywheel performance. Both designs assumed a composite banding stack-up consisting of 9 individual 25 mm thick composite rings, starting at an initial build radius of 175 mm. The composite bandings consisted of a mixture of IM7 and T1000, which has an average density of 1560 kg/m^3 and hoop strain limit of 1%. Both designs assumed the permanent magnet banding was 20 mm thick in the radial direction. The first design assumed a conventional permanent magnet array, which had high modulus in the radial direction, E_r, but very little in the hoop direction, E_t, as shown in Table 1. The second design assumed properties for an advanced magnetic composite that replicates the mechanical performance of S-Glass composite, with a density slightly less than a conventional magnet.

Table 1: Material properties for composite flywheel designs with bearing materials

	Er [GPa]	Et [GPa]	nu_rt	nu_tr	Den. [kg/m^3]
IM7 Composite	8.8	153.4	0.022	0.3824	1564
T1000 Composite	8.86	187.6	0.0183	0.3869	1561
Conventional Magnet	179.3	6.9	0.299	0.0115	7470
Magnetic Composite	20	50	0.1	0.2	7000

An optimization routine was performed with a 1-D nested ring analysis to determine optimal interference fits and maximum speeds for the conventional magnetic, and composite magnetic flywheel designs. Table 2 shows performance results for both design variants. Figure 9 plots the radial and hoop stress throughout the bandings of both design variants. Due to potential creep, the maximal compressive stress that the composite material can withstand is limited to 83 MPa. This stress defines the operating limit which is reached in both designs, as shown in Figure 9. The composite bandings can withstand tensile hoop stresses up to 1800 MPa, which are not approached in either design. Both of these designs are limited due to the mass loading of the dense magnetic material. As shown in Table 2, the magnetic composite, with increased hoop modulus and slightly lower density, allows the flywheel to reach higher maximum operating speeds. These higher speeds increase the specific energies by about 45%, volumetrically and per mass.

Table 2: Results from nested ring analysis showing performance improvement with bearing design using magnetically filled composite

	Omega [rpm]	Vtip [m/s]	Specific Energy [Wh/kg]	Vol. Energy [kWh/m^3]
Conventional Magnet	18,247	761.2	41.36	65.46
Magnetic Composite	21,988	915.3	60.37	94.66

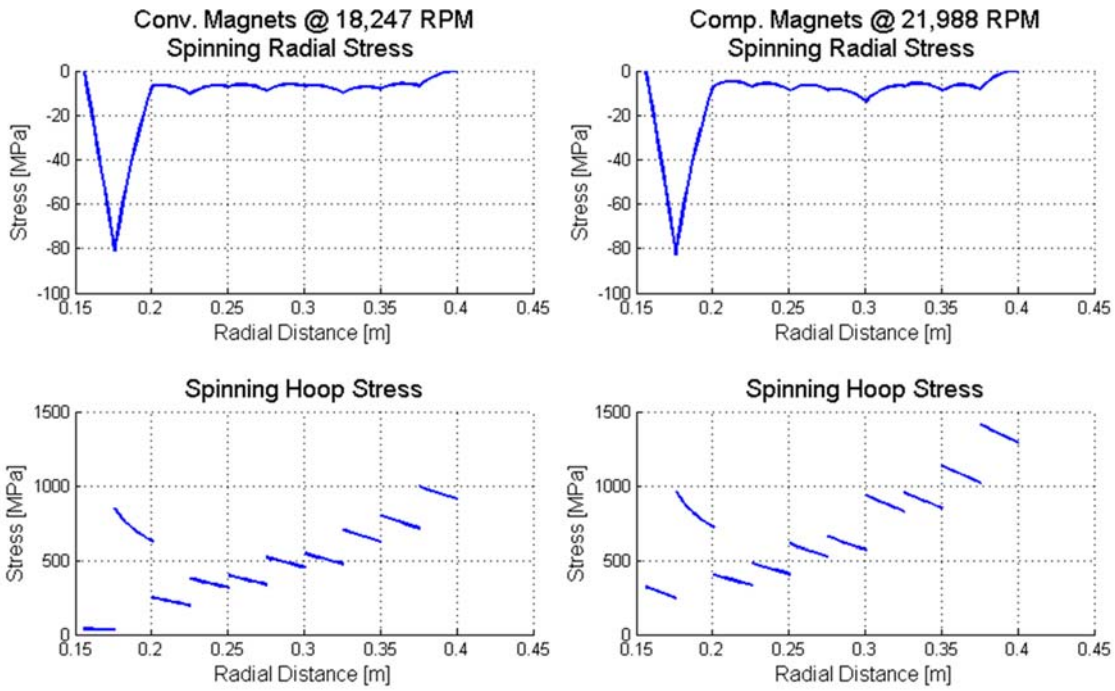

Figure 9: Nested ring analysis results; Right: Flywheel with conventional permanent magnet segments on bore ID. Left: Flywheel with magnetically filled composite on bore ID

Summary

Over the course of the GCEP program, UT-CEM, in partnership with UTD focused on developing design improvements for flywheel energy storage. Compared to electrochemical batteries, flywheels offer superior life cycle capabilities that can exceed 1 million full speed cycles. Improvements for flywheel energy storage must address the low specific energy and leakage losses that are primarily a resultant of bearing losses. The work performed by UT-CEM and UTD shows that both of these issues can be addressed by employing ultra-low loss high temperature superconducting bearings with magnetically filled composite materials. Flywheels using high temperature superconducting bearings can have loss rates as low as 0.1% per hour. To aid in these designs, UT-CEM developed lumped parameter modeling techniques for sizing high temperature superconducting bearings. Studies using these techniques show that improvements to specific and volumetric energy storage densities can be attained with magnetically filled composites, even if these composites have significantly lower field strength than standard high grade neodymium permanent magnets. These improvements result from the superior mechanical strength and hoop load carrying capability that the magnetic composites would have.

Publications

1. C.S. Hearn, M.C. Lewis, S.B. Pratap, R.E. Hebner, F.M. Uriate, D. Chen, and R.G. Longoria. "Utilization of Optimal Control Law to Size Grid-Level Flywheel Energy Storage." IEEE Transactions on Sustainable Energy. Vol.4, Is. 3, pp. 611-618, July 2013.
2. C.S. Hearn, S.B. Pratap, D. Chen, and R.G. Longoria, "Reduced Order Dynamic Model of Permanent Magnet and HTSC Interaction in an Axisymmetric Frame," IEEE Transactions on Mechatronics, Vol. PP, Is. 99, pp. 1-8, August, 2013.
3. C.S. Hearn, S.B. Pratap, D. Chen, and R.G. Longoria, "Lumped Parameter Model to Describe Dynamic Translational Interaction for High Temperature Superconducting Bearings," IEEE Transactions on Applied Superconductivity, Vol. 24, Is. 2, 3600808, April, 2014.
4. S.B. Pratap, C.S. Hearn, "3D Transient Modeling of Bulk High Temperature Superconducting Material in Passive Magnetic Bearing Applications," *submitted to* IEEE Transactions on Applied Superconductivity, Dec 2013.
5. C.S. Hearn, S.B. Pratap, D. Chen, and R.G. Longoria, " Dynamic Performance of Lumped Parameter Model for Superconducting Levitation," *submitted to* IEEE Transactions on Applied Superconductivity, March 26, 2014.

References

[1] M. L. Lazarewicz and T. M. Ryan, "Integration of flywheel based energy storage for frequency regulation on deregulated markets," in *Power and Energy Society General Meeting*, July 2010.

[2] B. T. Murphy, H. Ouroua, M. T. Caprio and J. D. Herbst, "Permanent Magnet Bias Homopolar Magnetic Bearings for a 130 kW-hr Composite Flywheel," in *The Ninth International Symposium on Magnetic Bearings*, Lexington, KY, Aug. 3-6, 2004.

[3] M. A. Pichot, J. P. Kajs, B. R. Murphy, A. Ouroua, B. M. Rech, R. J. Hayes, J. H. Beno, G. D. Buckner and A. B. Palazzolo, "Active Magnetic Bearings for Energy Storage Systems for Combat Vehicles," *IEEE Transactions on Magnetics*, vol. 37, no. 1, pp. 318-323, January 2001.

[4] M. Strasik, P. E. Johnson, A. C. Day, J. Mittleider, M. D. Higgins, J. Edwards, J. R. Schindler, K. E. McCrary, C. R. McIver, D. Carlson, J. F. Gonder and J. R. Hull, "Design, Fabrication, and Test of a 5-kWh/100-kW Flywheel Energy Storage Utilizing a High-Temperature Superconducting Bearing," *IEEE Transactions on Applied Superconductivity*, vol. 17, no. 2, pp. 2133-2137, June 2007.

[5] A. C. Day, J. R. Hull, M. Strasik, P. E. Johnson, K. E. McCrary, J. Edwards, J. A. Mittleider, J. R. Schindler, R. A. Hawkins and M. L. Yoder, "Temperature and Frequency Effects in a High-Performance Superconducting Bearing," *IEEE Transactions on Applied Superconductivity*, vol. 13, no. 2, pp. 2179-2184, June 2003.

[6] F. N. Werfel, U. Floegel-Delor, R. Rothfeld, T. Riedel, B. Goebel, D. Wippich and P. Schirrmeister, "Superconducting bearings, flywheels, and transportation," *Superconducting Sci. Technol.*, vol. 25, no. 014007, p. 16pp, 2012.

[7] T. A. Coombs, A. Cansiz and A. M. Campbell, "A superconducting thrust-bearing system for an energy storage flywheel," *Supercond. Sci. Technol.*, vol. 15, pp. 831-836, 2002.

[8] G. G. Sotelo, A. C. Ferreira and J. R. de Andrade, "Halbach Array Superconducting Magnetic Bearing for a Flywheel Energy Storage System," *IEEE Transactions on Applied Superconductivity*, vol. 15, no. 2, pp. 2253 - 2256, June 2005.

[9] M. Ikeda, A. Wongsatanawarid, H. Seki and M. Murakami, "Interaction of bulk superconductors with flywheel rings made of simple permanent magnets," *Physica C*, vol. 469, pp. 1270-1273, 2009.

[10] Y. H. Han, J. R. Hull, S. C. Han, N. H. Jeong, T. H. Sung and N. Kwangsoo, "Design and Characteristics of a Superconducting Bearing," *IEEE Transactions on Applied Superconductivity*, vol. 15, no. 2, pp. 2249-2252, June 2005.

[11] C.S. Hearn, S.B. Pratap, D. Chen, and R.G. Longoria, "Reduced Order Dynamic Model of Permanent Magnet and HTSC Interaction in an Axisymmetric Frame," IEEE Transactions on Mechatronics, Vol. PP, Is. 99, pp. 1-8, August, 2013.

Contacts

Dr. Robert Hebner: r.hebner@cem.utexas.edu
Dr. Siddharth Pratap: s.pratap@cem.utexas.edu
Mr. Michael Lewis: mclewis@cem.utexas.edu
Dr. Clay Hearn: hearn@cem.utexas.edu